# A test of the interstellar dust model of comets

Greenberg, J.M.; Hage, J.I.

# A TEST OF THE INTERSTELLAR DUST MODEL OF COMETS

## J M Greenberg & J I Hage

*Astrophysics Laboratory, University of Leiden, The Netherlands*

ABSTRACT

The interstellar dust model of comets is used as a basis to simultaneously satisfy various observational constraints and to derive the porosity of comet dust. The observational constraints are : (1) the strengths of the 3.4 $\mu m$ and 9.7 $\mu m$ emission bands ; (2) the shape of the 9.7 $\mu m$ band; (3) the relative amount of silicates to organic materials ; (4) the mass distribution of the dust. The method used involves precise calculation of the temperatures and emission characteristics of porous aggregates of interstellar dust as a function of their mass, porosity and distance to the sun and the wavelength. The results indicate a high porosity of comet dust.

Keywords : coma dust, infrared spectra, interstellar grains.

## 1 INTRODUCTION

The basic idea of the interstellar dust model of comets by Greenberg (1982, 1985) is that in the regions of the protosolar nebula where comets were born the temperature was so low that all components of the dust were preserved during aggregation into a comet. It has been proposed by Greenberg (1986) that during the formation of comets, aggregates of interstellar dust particles are made as illustrated schematically in figure 1. The individual interstellar dust grains contain a core of interstellar silicate and a mantle of organic refractory material. The aggregates are expected to have a packing factor of $\approx$ 0.2 (this corresponds to 80% vacuum, or porosity $P = 0.8$). The tangled structure of these aggregates, like a bird's nest, is suggested as a possible way to provide them with rigidity. The aggregates, in turn, coalesce to form much larger bodies and ultimately comets. When a comet comes close to the sun, the particles in the coma, which have been lifted from the comet surface, must initially consist of such fluffy aggregates of various sizes, with a porosity of about 0.8. The outer icy mantles (predominantly $H_2O$) evaporate quickly (close enough to the sun) once an individual aggregate is lifted from the comet and is fully exposed to the solar radiation. After evaporation of these volatile ices the aggregates consist of sub-micron particles $(m \approx 6 \times 10^{-14} g)$ composed of organic refractory material and interstellar silicates. The predicted porosity of the coma dust is $P \approx 0.95$.

In this paper we use the interstellar dust model as a basis to quantitatively explain ground based infrared observations of the inner coma of comet Halley around $\lambda = 3.4 \mu m$ and $\lambda = 9.7 \mu m$ in terms of the particle size distributions measured in situ by the Giotto and Vega missions. At the same time we satisfy the relative amounts of organic and silicate material required by Giotto mass spectroscopy observations (Kissel and Krueger, [1987]). When an earlier attempt was made (Greenberg, et. al., 1989), it was found that the amount of small particles required to explain the infrared observations was between one and two orders of magnitude higher than then believed to exist (McDonnell et. al., 1987). The present paper uses the results of the improved calibration of the PIA and DIDSY instruments (McDonnell et. al., [1989]), VEGA mass spectrometer data (Mazets et. al. 1987) and rigorous calculations of the temperatures and spectral properties of porous aggregates of interstellar dust to derive information about the porosity of the coma dust. The organisation of this paper is as follows. In section 2a formulae are derived which show the relation between the observed size spectra in the coma and observations of the thermal emission. Section 2b lists our choice of observational results. In section 3 and 4 we derive the emission properties and temperatures of porous aggregates of interstellar dust as a function of their size, porosity and composition. In section 5 the results of sections 2, 3 and 4 are used to derive the porosity of the dust in the coma of comet Halley. Section 6 contains a discussion and our conclusions.
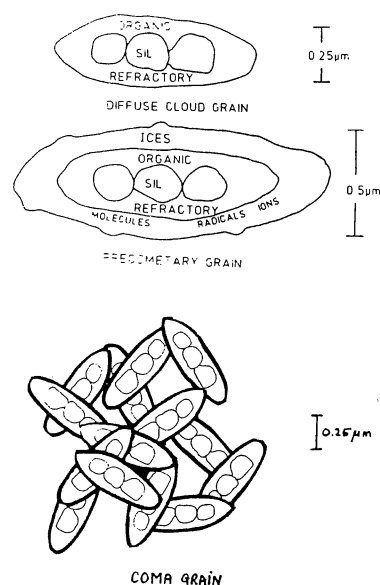


**Figure 1.** Top: Schematic of an interstellar dust grain, which contains a core of silicates and a mantle of organic refractory material. Middle: An interstellar grain as it would appear in the presolar dust cloud after accretion of gases on its surface. These grains make up a comet. Bottom: Schematic of a coma grain as it would appear according to the interstellar dust model. It would have a porosity of about 95%.

## 2 METHOD.

### 2a Theory

For the purpose of our discussion, we consider the coma of comet Halley to be a spherically symmetric cloud of gas and dust, in which the particle density decreases as the inverse square of the distance to the comet nucleus. We shall assume that the outward flow of dust particles is directed radially from the nucleus and that the particle mass spectrum does not depend on the distance to the nucleus in the inner coma. Let the flux (per unit wavelength) observed at earth from the coma, seen within an aperture defined by a radius $R_a$ at the comet, be denoted by $F(\lambda)$. Then the total power, $W^\circ$ emitted in all directions from the central spherical region within the aperture is

$$W^\circ = \frac{2}{3} 4\pi \Delta^2 F(\lambda) \quad , \tag{1}$$

where $\Delta$ is the distance from the Earth to the comet at the time of observation. The factor 2/3 takes into account to a good approximation

that the emission as seen from Earth comes from a cylindrical volume rather than from a sphere.

We define the mass absorption coefficient of a particle, $\kappa(\lambda)$, as

$$\kappa(\lambda) = \frac{C_{\text{abs}}(\lambda)}{M} \quad , \qquad (2)$$

where $C_{\text{abs}}$ is the cross section for absorption of the particle and $M$ its mass. The emitted power by a spherical particle at a temperature, $T$, is then given by the product $4\pi M \kappa(\lambda) B(\lambda, T)$, where $B(\lambda, T)$ is the Planck function. In terms of the particles in the observed central spherical part of the coma, assuming that particles with the same mass are identical, the total emitted power per unit wavelength, $W^e$, is

$$W^e = 4\pi \left(4\pi R_a^3\right) \int_0^\infty \kappa(\lambda) B(\lambda, T) M \, n(M) \mathrm{d}M \quad , \qquad (3)$$

where $n(M)\mathrm{d}M$ is the number of particles of mass $M$ per unit volume at a distance $R_a$ from the comet, in the mass range $\mathrm{d}M$. A theoretical fit of the observed spectrum must therefore satisfy

$$4\pi R_a^3 \int_0^\infty \kappa(\lambda) B(\lambda, T) M \, n(M) \mathrm{d}M = \frac{2}{3} \Delta^2 F(\lambda) \quad , \qquad (4)$$

for all wavelengths where the thermal emission dominates the reflected solar radiation.

Basic to this work is the consideration of the emission bands at 3.4 $\mu m$ and 9.7 $\mu m$, which appear clearly above the continuum radiation from the coma. For either of these bands we define the excess emission above the continuum, $F^{ex}$, as

$$F^{ex}(\lambda) = F(\lambda) - \left[ F(\lambda_1) + \frac{F(\lambda_2) - F(\lambda_1)}{\lambda_2 - \lambda_1}(\lambda - \lambda_1) \right] \quad . \qquad (5)$$

Here $\lambda_1$ and $\lambda_2$ are the lower and upper wavelenghts of the bands, respectively. If we also define the effective mass absorption coefficient for a particle and for these bands, $\kappa^{eff}$, as

$$\kappa^{eff}(\lambda) = \frac{C_{\text{abs}}(\lambda) - \left[ C_{\text{abs}}(\lambda_1) + \frac{C_{\text{abs}}(\lambda_2) - C_{\text{abs}}(\lambda_1)}{\lambda_2 - \lambda_1}(\lambda - \lambda_1) \right]}{M} \quad , \qquad (6)$$

then, if there is a well defined emission band between $\lambda_1$ and $\lambda_2$, equation (4) becomes, to a good approximation :

$$4\pi R_a^3 \int_0^\infty \kappa^{eff}(\lambda_p) B(\lambda_p, T) M \, n(M) \mathrm{d}M = \frac{2}{3} \Delta^2 F^{ex}(\lambda_p) = W^{ex}/4\pi, \qquad (7)$$

for $\lambda_1 < \lambda_p < \lambda_2$. Here $\lambda_p$ denotes the wavelength of the band peak. This approximation breaks down in case the Planck function has a sharper peak than $\kappa^{eff}$, which is, however, not the case we are interested in. Equation (7) shows how the relation between two observed quantities, $F^{ex}(\lambda)$ and $n(M)$, depends on the properties of the emitting dust, through the quantities $\kappa^{eff}$ and $T$.

In this paper we shall assume that the coma dust has a certain porosity which is unknown, and which must therefore be taken as a free parameter in the calculations of the coma dust emission. The goal of this work is to calculate the left hand side of equation (7) as a function of porosity of the coma dust and then, by equating left and right hand sides, using equation (7) to determine the porosity of the coma dust. In particular, we shall satisfy equation (7) for the 3.4 $\mu m$ and 9.7 $\mu m$ bands. We shall calculate the quantities $\kappa^{eff}$ and $T$ of the coma dust particles exactly, based on the composition and structure of coma dust as derived from the interstellar dust model. The dependence of $\kappa^{eff}$ and $T$ on particle size (or mass $M$), particle porosity ($P$), wavelength ($\lambda$) and distance to the sun ($r$) will be taken fully into account. Furthermore, we use for $n(M)$ the dust mass spectra as measured in situ by the spacecraft missions to comet Halley, thus implicitly satisfying one observational constraint. The mean size of the individual interstellar grains in the coma particles follows from the interstellar dust model and is fixed at 0.2 $\mu m$. Lastly, the relative size of the core and mantle are taken so that the mass ratio of the silicates to organic material is 2:1, thus satisfying another observational constraint (Kissel and Krueger, 1987). In sections 3 and 4, the calculation of $\kappa^{eff}(\lambda, P, M)$ and $T(P, M, r)$ is discussed in more detail.

### 2.b Observations

Because of variability in the dust emission, it is necessary to choose observations of $n(M)$ and $F^{ex}(\lambda)$ as close together in time as possible. The Vega1, Vega2 and Giotto closest approaches occurred on March 6, 9 and 14 respectively. We have chosen to use the observations by Hanner *et. al.* (1987 ) on March 6.85, 12.8 and 13.75 . For use in

equation 5, $\lambda_1 = 7.8\mu m$, and $\lambda_2 = 12.5$ for these observations. As far as we know no observations of the 3.4 $\mu m$ band were done on these days. Therefore we have taken observations at a later date (March 28) to obtain the ratio of the 9.7 $\mu m$ excess to the 3.4 $\mu m$ excess and we use this ratio to estimate the value of $F^{ex}(3.4)$ on March 6.85, 12.8 and 13.75. The value deduced from observations on March 28.6 by Gehrz and Ney (1986) is $F^{ex}(9.7) = 1.2 \times 10^{-16} W\ cm^{-2}\mu m^{-1}$ . The value for $F^{ex}(3.4)$ from Danks *et. al.* is $F^{ex}(3.4) = 2.6 \times 10^{-17} W\ cm^{-2}\mu m^{-1}$ . After normalising these values to a single aperture, we obtain a ratio of about 10. However, we note that the measurements by Gehrz and Ney did not include the 7.8 $\mu m$ filter, so that we used $\lambda_1 = 8.5\mu m$ in equation 5 instead, thereby underestimating the strength of the 9.7 $\mu m$ band. We shall therefore assume $F^{ex}(9.7)/F^{ex}(3.4) > 10$ on March 6.85, 12.8 and 13.75.

The quantity $n(M)$ may be obtained from the cumulative particle fluxes measured by the spacecraft by differentiating the cumulative fluxes and dividing the result by the spacecraft velocity. We have used the results presented in figure 1 of McDonnell *et. al.* (1989) to derive $n(M)$ for the Giotto passage on March 14. We note that due to a recalibration of the instruments, the $n(M)$ for $10^{-15}g < M < 10^{-10}g$ deduced from this are a factor of up to 25 times larger than the values that would be deduced from the results as presented in McDonnell *et. al.* (1987). We obtained $n(M)$ for the Vega missions from Mazets *et. al.* (1987) (their figures 5 and 8, top curves). We note that the Vega and Giotto differential particle mass distributions are similar up to masses of about $1 \times 10^{-9}g$, but that differences of up to two orders of magnitude occur in the differential amount of mass for the higher masses.

### 3 MASS ABSORPTION COEFFICIENTS.

#### 3a Optical Constants.

The mass absorption coefficients $\kappa(\lambda)$ and $\kappa^{eff}(\lambda)$ depend on the dust material (through the optical constants), and the morphology and size parameter of the particles. The size parameter is defined as

$$x = \frac{2\pi a}{\lambda} \quad , \qquad (8)$$

where $a$ is a typical particle dimension. In the case of a sphere, for example, $a$ would be the radius. For the silicates, we use the optical constants as presented by Draine and Lee (1984) for "astronomical silicates" . An important feature of this material is its strong 9.7 $\mu m$ band, which we use to model the emission of comet Halley at this wavelength.

The optical constants of the organic refractories are adopted from the values given by Chlewicki and Greenberg (1989). These are based in part on laboratory measurements of the residues of ice mixtures irradiated with ultraviolet light. The visible properties of the organic refractory are consistent with the observed albedo, linear and the circular polarization of silicate core-organic refractory interstellar particles. There are two main features of this material with respect to the present paper : (1) the emission band at 3.4 $\mu m$, with which we represent the emission feature of comet Halley at around this wavelength, and (2) the absorptivity in the visual which is much higher than the absorptivity of the astronomical silicate in this wavelength region. This causes the dust in the coma of Halley which contains organic material to be hotter than purely silicate dust.

#### 3.b Effect of Size and Morphology

Figure 2 shows the shape of the 9.7 $\mu m$ silicate band as it is emitted by purely silicate spheres of various sizes. From figure (2) it is clear that in order for a silicate sphere to emit (or absorb) effectively above the continuum at a wavelength $\lambda_p \approx 9.7\mu m$ it must satisfy approximately $a \leq 1\mu m$. For the larger spheres the absorption shape is distorted and $\kappa^{eff}$ is low. Therefore, for $\lambda_p = 9.7\mu m$, only those *solid* silicate particles with a characteristic size smaller than about $1\mu m$ will contribute effectively to the 9.7$\mu m$ *excess* to the comet emission.

To calculate $\kappa^{eff}$ of porous aggregates we represent aggregates of interstellar dust, such as could have been present in the coma of comet Halley (c.f. figure 1), as a collection of identical particles with a fixed size, which may be either randomly situated and loosely bound to each other or more closely packed. The overall shape of the aggregate is taken as spherical. The parameters describing such an aggregate are its radius, $R$, the refractive index, $m$, size, $a$, and shape of its constituent particles, and its fluffiness, or porosity, $P$. The porosity $P$ is defined as the fractional amount of vacuum within the aggregate :

$$P = 1 - \frac{V_{\text{solid}}}{V} \quad , \qquad (9)$$

where $V$ is the total volume of the aggregate, defined by the smallest spherical surface which completely surrounds the whole aggregate and $V_{\text{solid}}$ is the amount of solid material inside this bounding surface. We have $0 \leq P < 1$, where $P = 0$ corresponds to a solid aggregate and $P \approx 1$ corresponds to a cloud of independent particles.
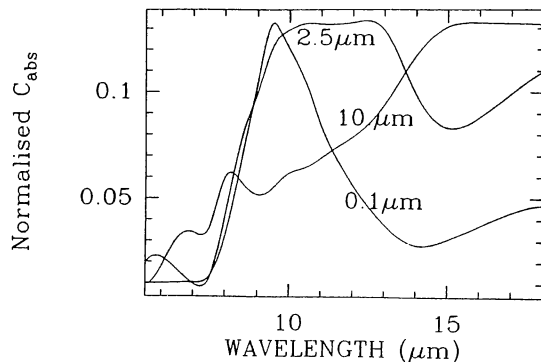
**Figure 2.** Normalised values of the cross section for absorption of purely silicate spheres. The curves apply to spheres with radii of 0.1 $\mu m$, 2.5 $\mu m$ and 10 $\mu m$. Clearly small particles emit the 9.7 $\mu m$ better than large particles.



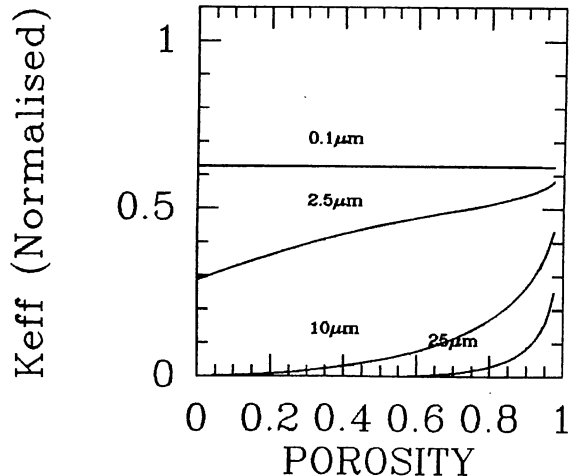**Figure 3.** The normalised mass absorption coefficients at $\lambda = 9.7\mu m$ for coma dust as a function of the dust porosity and size. The labels indicate the radius of the aggregate at zero porosity. A single curve applies to a particle of constant mass. The values shown are ratioed to $\kappa^{\text{eff}}(9.7)$ of small, purely silicate particles.

It is shown by Hage and Greenberg (1989) that if the inclusions are homogeneous and satisfy $x \ll 1$, the absorption cross sections of the aggregates described above can be determined by calculating an effective refractive index for the whole aggregate and subsequently using Mie scattering theory to obtain the various cross sections. The effective refractive index of the aggregate, $m_{\text{av}}$, is calculated according to the Maxwell-Garnett effective medium theory (Maxwell-Garnett, [1903], to be called Maxwell-Garnett EMT hereafter), with vacuum as the so-called "matrix" material and the individual particles as the "inclusions". The effective refractive index thus obtained depends on the porosity and is given by

$$m^2_{\text{av}} = 1 + \frac{3(1-P)(m^2-1)/(m^2+2)}{1-(1-P)(m^2-1)/(m^2+2)}, \quad (10)$$

where $m$ is the refractive index of the inclusions.

Since we assume that the inclusions are individual interstellar dust grains, which at $3.4\mu m$ and at $9.7\mu m$ satisfy $x \ll 1$ we may apply the above procedure. To apply the above method also to aggregates consisting of inhomogeneous particles such as interstellar dust grains, we describe these constituent particles as core-mantle spheres with an effective refractive index $m^i_{\text{av}}$, using the core as "inclusion" and the mantle as "matrix" material. The effective refractive index for the constituent particles thus defined is

$$(m^i_{\text{av}})^2 = m^2_2 \left[ 1 + 3q^3 \left( \frac{m^2_2 - m^2_1}{m^2_2 + 2m^2_1} \right) \left\{ 1 - q^3 \left( \frac{m^2_2 - m^2_1}{m^2_2 + 2m^2_1} \right) \right\}^{-1} \right] \quad , \quad (11)$$

where $a$ is the radius of the constituent particle, $q$ and $m_2$ the fractional radius and refractive index of its core, and $m_1$ the refractive index of its mantle. This approach is justified because the polarizability of the core-mantle spheres (which completely determines their scattering properties) implied by equation (11) is exactly correct for concentric core-mantle spheres in the limit $x \to 0$. The effective refractive index given by equation (11) is to be used in the right hand side of equation (10) to obtain the effective refractive index of the aggregate as a whole.

Figure 3 shows $\kappa^{\text{eff}}(9.7)$ of the coma dust particles as a function of their porosity and size. The values shown are ratioed to $\kappa^{\text{eff}}(9.7)$ of purely silicate particles with $x \ll 1$. The labels correspond to the aggregate radii at $P = 1$. For example, an aggregate with porosity $P$ containing the same amount of material as a solid aggregate with a radius of $R$, has a radius of $a = R/(1-P)^{1/3} = 32\mu m$ for $P = .97$ and $R = 10\mu m$.

Figure 3 shows that, at a certain porosity, $\kappa^{\text{eff}}(9.7)$ decreases as the particle size increases. Note how rapidly the effective absorption drops for solid particles $(P = 0)$: from 0.1 to 2.5 $\mu m$ the reduction is about $1/2$, and for 10 $\mu m$ $\kappa^{\text{eff}} \approx 0$. At a given size (but greater than approximately 2 $\mu m$), $\kappa^{\text{eff}}(9.7)$ increases as the porosity increases. In the limit $P \to 1$, all aggregates have an effective mass absorption coefficient as high as that of a small particle. Furthermore, for sufficiently high porosities, the shape of the absorption as a function of wavelength is like that of a small particle and not distorted as in figure 2 (see Hage and Greenberg, 1989).

### 4 DUST TEMPERATURES

We have used the following standard equation to calculate the temperature of a spherical body in a radiation held

$$\int_0^\infty C_{\text{abs}}(\lambda) F_r(\lambda) d\lambda = 4\pi \int_0^\infty C_{\text{abs}}(\lambda) B(\lambda, T) d\lambda \quad . \quad (12)$$

Here $F_r$ denotes the ambient radiation field, $C_{\text{abs}}$ and $T$ are the absorption cross section and temperature of the dust particle respectively. Equation (12) expresses the fact that in equilibrium with the radiation field, a body emits the same amount of energy as thermal emission as it absorbs at other wavelengths. Let us first consider a few special limiting cases: (1) absorbing particles which are relatively large, will have $Q_{\text{abs}}(\lambda) \approx 1$ for a large range in $\lambda$, so that they will approximately have the temperature of a black body, $T \approx 279r^{-0.5}$, where $r$ is the distance to the sun, in astronomical units; (2) individual core- mantle dust particles with a typical size of e.g. a few tenths of a micrometer will be much hotter, because they emit relatively poorly in the infrared (since $C_{\text{abs}} \sim 2\pi/\lambda$), but absorb well in the visual and ultraviolet; (3) lastly, the temperature attained by an aggregate in the limit $P \to 1$ is equal to the temperature of a single inclusion as if it were exposed to the radiation field on its own. This is because the inclusions in very porous aggregates do not shadow each other much and absorb and emit radiation nearly as if independent of each other. In general, the temperature of an aggregate depends on its distance to the sun, on its size and fluffiness and on the properties of the individual constituents.

To satisfy equation (12) for a certain particle in practice, one has to calculate the emitted power for a range of temperatures, calculate the absorbed power and then interpolate to match emission and absorption and find the correct particle temperature (see, e.g. Greenberg, 1971). To calculate the absorption cross sections for the solid particles, we have used the standard Mie theory. For solid core-mantle particles, we have used another appropriate version of the Mie-theory. As far as the aggregates are concerned, we may only use the combined Mie theory–Maxwell-Garnett EMT approach to calculate their absorption cross sections if $x \ll 1$ for the individual constituents. Since the individual constituents are interstellar dust grains with a radius of about 0.1 $\mu m$, this approach is valid up to $\lambda \approx 1\mu m$. For shorter wavelengths, we consider these aggregates to have the optical characteristics of a cloud of independent particles. This approximation works well if $X > 10$. The mean optical depth, $\tau$, of a spherical cloud of identical small $(x \ll 1)$, absorbing particles is given by

$$\tau \approx NRC^i_{\text{abs}} \quad (13)$$

where $N$ is the number of particles per unit volume, $R$ the radius of the cloud and $C^i_{\text{abs}}$ the cross section for absorption of an individual particle. To a first approximation, the flux of a plane wave incident on such a cloud is reduced by a factor $e^{-\tau}$. In this approximation, the absorption cross section of the aggregate is

$$C_{\text{abs}} = G(1 - e^{-\frac{4}{3}\tau}), \quad (14)$$

where G is the geometrical cross section of the cloud $(G = \pi R^2)$ and the factor $\frac{4}{3}$ is inserted to give the correct value for limit $P \to 1$, the limiting value being the sum of the absorptions by all constituent particles.

Results for the temperatures of the aggregates as a function of porosity and size are shown in figure 4. The temperatures shown are computed for a solar distance of $0.9 AU$. In general, the trends discussed above are borne out by the results of the exact calculations used to draw figure 4. Note that the rise in temperature to the limiting value does not become rapid until quite high values of P.
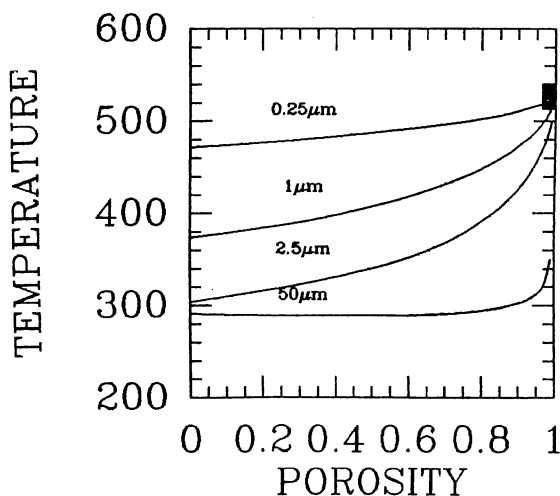
**Figure 4.** The temperature of coma dust as a function of the dust porosity and size. The labels indicate the radius of the aggregate at zero porosity. A single curve applies to a particle of constant mass. The filled square is the limiting temperature of a single interstellar grain.



**Figure 5.** The power per unit wavelength at 9.7 $\mu m$ emitted from coma of Halley calculated using equation (7), as a function of the porosity of the coma dust. Long dashes : the power emitted from the spherical region around the nucleus with a radius of 5620 km on March 6.85, using the particle size distribution measured by Vega1. Short dashes : the power emitted from the spherical region around the nucleus with a radius of 4900 km on March 12.8, using the particle size distribution measured by Vega2. Continuous line : the power emitted from the spherical region around the nucleus with a radius of 4900 km on March 12.8, using the particle size distribution measured by Giotto.

## 5 RESULTS

Figure 5 shows the theoretical emission from comet Halley's coma at 9.7$\mu m$ in Watts per centimeter, as a function of the porosity of the coma particles, calculated using equation (7) and the methods described in sections 3 and 4. The line with the long dashes shows the emission expected from the coma in an aperture corresponding to 5620 km at the comet nucleus on March 6.85, using the particle mass spectrum measured by Vega1. The short- dashed and continuous lines show the emission from the coma in an aperture corresponding to 4900 km at the nucleus on March 12.8, using mass spectra measured by Vega2 and Giotto, respectively. Figure (6) shows the same set of curves, but now for the emission at 3.4$\mu m$.

We may use the observed values of $F^{ex}(9.7)$ on the corresponding dates, and the observed value of the ratio $F^{ex}(9.7)/F^{ex}(3.4) > 10$ on March 28 to read the required porosities from these figures, in order to satisfy equation (7). Table 1 shows the results obtained, including results of identical calculations and observations on March 13.75.

After having thus found the porosity necessary to fit the amount of excess emission, it is possible to compute the shape of the 9.7$\mu m$ band also, using the values for the porosity obtained from figure 5. The curve in figure 7 shows the result for the band shape on March 12.8, using a porosity of about 0.85 and the Giotto size distribution. The crosses in this figure represent ground based observations on this date, by Hanner *et. al.*, (1987). Figure 7 shows that a reasonable match is obtained. However, using $P \approx 0.4$ and the Vega1 mass spectrum, the resulting bandwidth is about 50% too wide compared to the observations by Hanner *et. al.* on March 6.85 (see figure 8). The Vega2 mass spectrum gives a bandwidth which is about 30% too wide on March 12.8 .
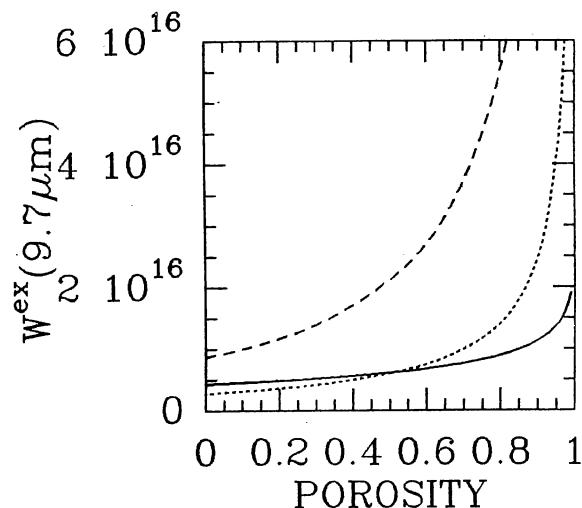


**Figure 6.** The power per unit wavelength at 3.4 $\mu m$ emitted from coma of Halley calculated using equation (7), as a function of the porosity of the coma dust. Long dashes : the power emitted from the spherical region around the nucleus with a radius of 5620 km on March 6.85, using the particle size distribution measured by Vega1. Short dashes : the power emitted from the spherical region around the nucleus with a radius of 4900 km on March 12.8, using the particle size distribution measured by Vega2. Continuous line : the power emitted from the spherical region around the nucleus with a radius of 4900 km on March 12.8, using the particle size distribution measured by Giotto.
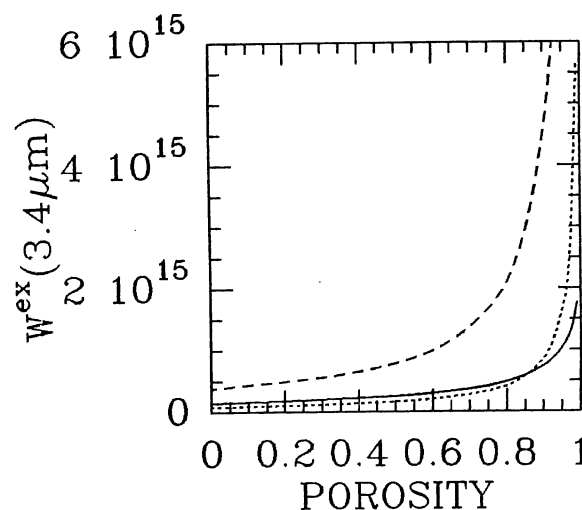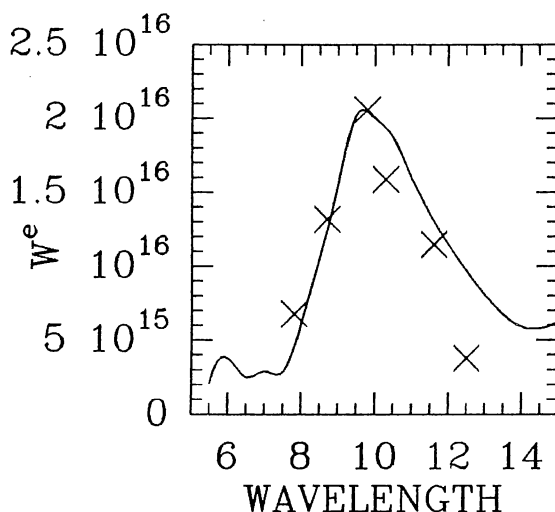
| Date | $n(M)$ | $P(9.7)$ | $P(3.4)$ |
|---|---|---|---|
| March 6.85 | Vega1 | 0.40 | < 0.75 |
| March 12.8 | Vega2 | 0.70 | < 0.90 |
| March 12.8 | Giotto | 0.85 | < 0.95 |
| March 13.75 | Giotto | 0.55 | < 0.875 |

**Table 1.** The porosity of the coma dust derived by application of equation (7). $P(9.7)$ is the porosity required to match the strength of the 9.7 $\mu m$ emission band, and $P(3.4)$ is the result for the 3.4 $\mu m$ band.

Figure 7. The shape of the 9.7 $\mu m$ band calculated using equation (3), using the Giotto dust size distribution and a porosity of $P \approx$ 0.85. The crosses show the observations by Hanner *et. al.* on March 12.8 .
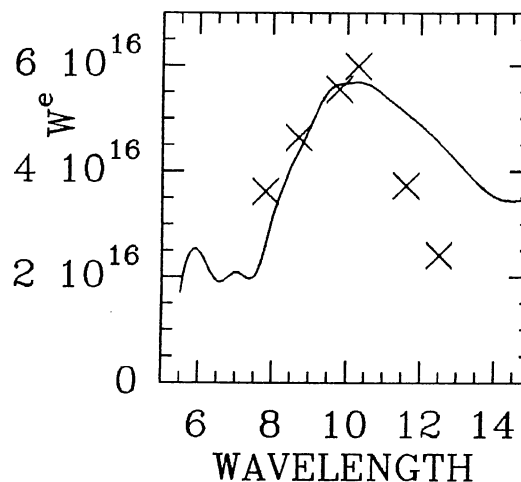


Figure 8. The shape of the 9.7 $\mu m$ band calculated using equation (3), using the Vega1 dust size distribution and a porosity of $P \approx$ 0.4. The crosses show the observations by Hanner *et. al.* on March 6.85

## 6 DISCUSSION AND CONCLUSIONS

Table 1 shows that the interstellar dust model of comets is able to provide the basis to quantitatively and simultaneously satisfy the observational constraints of: (1) the particle mass spectra; (2) the mass ratio of organic to silicate material in the coma dust; (3) the absolute amount of excess emission in the 9.7$\mu m$ band; (4) the absolute amount of emission in the 3.4$\mu m$ band. The fact that the porosities required to match the 3.4$\mu m$ and the 9.7$\mu m$ bands on the same date are not too far apart gives confidence in the consistency of the model. However, although $P > 0$ is always consistently required, the result $P = 0.4$ obtained for March 6.85 and the Vega1 data is rather low compared with the predictions of the interstellar dust model. Furthermore, we do not expect variations from say, 0.4 to 0.85 in the porosity of the coma particles over a time span of a week. We may also include the band shape at 9.7$\mu m$ as another constraint in the discussion. Although the Giotto mass spectrum gives the correct band shape, the Vega mass spectra result in band shapes that are too wide. The 9.7$\mu m$ band shape is distorted only by the relatively large, low porosity particles (c.f. figure 2). If the porosities as deduced from the calculations using the Vega mass spectra were significantly higher, then these calculations would have given narrower bandshapes, but would also produce more emission in the 9.7 $\mu m$ band than observed. However, there are indications that we have over-estimated the amount of dust particles in the coma and that consequently the amount of theoretical emission from equation (7) is too high. Firstly, the mass spectra we have used have been measured in the sunward hemisphere of the coma, where the particle densities are known to be higher than on the night side of the comet. If we take the density on the dark side a factor three lower (as indicated by Giotto post- and pre- encounter data) then the theoretical amount of emission as given by equation (7) must be multiplied by 2/3. The resulting porosities read from a plot like figure 5 would therefore be higher. For example, the case for March 12.8, using the Giotto mass spectrum, now gives $P(9.7) = 0.97$ and $P(3.4) = 0.98$. Secondly, whereas the Giotto spectrum we have used is an average over a pathlength of about 4100 km (McDonnell *et. al.*, (1989), the Vega data we have used are apparently influenced more by the jet-like structure of the inner coma. Judging from figure 10 of Mazets *et. al.* (1987), it seems likely that the flux curves at closest approach for the Vega spacecraft (which we have used) are representative of the particle density within a jet, and thus give an overestimate of the average density. From the same figure we deduce that the average particle density may be lower by a factor of 2 than the actual density measured by the Vega1 spacecraft. For the Vega2 measurements, a factor of 1.5 seems applicable. Table 2 shows the porosities of the coma dust we find if these rough correction factors are taken into account. Assuming that the numbers in table 2 are correct we conclude that the coma dust has a porosity of at least 0.75, but more likely in the range 0.95 . These higher values improve the 9.7 $\mu m$ band shapes and are roughly consistent with the interstellar dust model. Finally, if the value of 0.95 applies to the coma dust we may reconstitute the volatiles into the dust to find the porosity and density of the comet itself. Based on the interstellar dust model this results in a comet porosity of 0.67 and a comet density of 0.51 $gcm^{-3}$. We note that this density is close to the value of 0.6 $gcm^{-3}$ found by Sagdeev *et. al.*, (1988).

| Date | $n(M)$ | $P(9.7)$ | $P(3.4)$ |
|------|--------|----------|----------|
| March 6.85 | Vega1 | 0.77 | < 0.90 |
| March 12.8 | Vega2 | 0.89 | < 0.97 |
| March 12.8 | Giotto | 0.97 | < 0.98 |
| March 13.75 | Giotto | 0.80 | < 0.94 |

Table 2. The porosity of the coma dust derived by application of equation (7), including corrections concerning the inhomogeneity of the coma dust distribution. $P(9.7)$ is the porosity required to match the strength of the 9.7 $\mu m$ emission band, and $P(3.4)$ is the result for the 3.4 $\mu m$ band.

### References

Chlewicki, G. and Greenberg, J.M. Astrophys. J. submitted (1988)

Danks, A.C., Encrenaz, T., Bouchet, P., LeBertre, T. and Chalabaeu, A., Astron. Astrophys. **184**, 329-332 (1987).

Draine, B.T. and Lee, H.M. Astrophys. J. **285**,89-108 (1984).

Gehrz, R.D. and Ney, E.P. in Proc. 20th ESLAB Symposium on the Exploration of Halley's Comet, ESA SP-250, 1010-105 (1986).

Greenberg, J.M., Nature, **321**, 385 (1986).

Greenberg, J. M., Zhao N. S. and Hage, J. I., (1989) Adv. Space Res. 9, no. 3, 3.

Greenberg, J. M., (1971), Astron. Astrophys. **12**, 204- 249.

Greenberg, J.M. in "Comets", ed. L.L. Wilkening, 131-163 (U. of Arizona Press, Tucson (1982)

Greenberg, J.M. Physica Scripta, **11**,14-26 (1985).

Hanner, M.S. Tokunaga, A.T., Golisch, W.E., Gripe, D.M. and Kaminski, C.D. Astron. Astrophys. **187**, 653-660 (1987).

Kissel, J. and Krueger, F.R. Nature, 326, 755-760 (1987).

Maxwell-Garnett, J. C., 1904, Phil. Trans. R. Soc. Lond., A203, 835.

Mazets E. P. *et. al*. Astron. Astrophys. 187, 699- 706, (1987).

McDonnell, J.A.M. *et. al*., Astron. Astrophys. 182, 719-714 (1987).

McDonnell, J.A.M. *et. al*., in: Workshop on Analysis of Returned Comet Nucleus Samples, Milpitas, California (1989).

Sagdeev, R. Z. *et. al*. Nature (1988),    331, p240-242.